Harmonically trapped four-boson system

D. Blume,[1] M. W. C. Sze,[2] and J. L. Bohn[2]

[1]*Homer L. Dodge Department of Physics and Astronomy, The University of Oklahoma, 440 W. Brooks Street, Norman, Oklahoma 73019, USA*

[2]*JILA, NIST, and Department of Physics, University of Colorado, Boulder, Colorado 80309-0440, USA*

(Received 31 January 2018; published 26 March 2018)

Four identical spinless bosons with purely attractive two-body short-range interactions and repulsive three-body interactions under external spherically symmetric harmonic confinement are considered. The repulsive three-body potential prevents the formation of deeply bound states with molecular character. The low-energy spectrum with vanishing orbital angular momentum and positive parity for infinitely large two-body s-wave scattering length is analyzed in detail. Using the three-body contact, states are classified as universal, quasiuniversal, or strongly nonuniversal. Connections with the zero-range interaction model are discussed. The energy spectrum is mapped out as a function of the two-body s-wave scattering length a_s, $a_s > 0$. In the weakly to medium-strongly interacting regime, one of the states approaches the energy obtained for a hard-core interaction model. This state is identified as the energetically lowest-lying "BEC state." Structural properties are also presented.

DOI: 10.1103/PhysRevA.97.033621

I. INTRODUCTION

The unitary two-component Fermi gas is realized when the s-wave scattering length a_s between the spin-up and spin-down atoms is infinitely large [1]. In the limit that the range of the interspecies interactions goes to zero, the unitary Fermi gas has been shown to be fully universal, i.e., the infinitely strongly interacting gas is characterized by the same number of length scales as the noninteracting gas [2–4]. The relevant length scales in the universal regime are the de Broglie wavelength and the average interparticle spacing that is related to the density of the homogeneous system [5]. For the harmonically confined system with angular frequency ω, the latter scale is typically replaced by the harmonic-oscillator length $a_{\rm ho}$, where $a_{\rm ho} = \sqrt{\hbar/(m\omega)}$. Here, m denotes the atom mass.

Universality implies that the realistic two-body interaction potentials can be replaced by a two-body boundary condition on the many-body wave function $\Psi_{\rm tot}$ in the limit that the interparticle distance coordinate r_{jk} of particle j (a spin-up atom) and particle k (a spin-down atom) goes to zero while all other coordinates $(\vec{r}_j + \vec{r}_k)/2$, $\vec{r}_1, \ldots, \vec{r}_{j-1}, \vec{r}_{j+1}, \ldots, \vec{r}_{k-1}, \vec{r}_{k+1}, \ldots, \vec{r}_N$ are being held fixed:

$$\lim_{r_{jk}\to 0} \frac{1}{r_{jk}\Psi_{\rm tot}} \frac{\partial(r_{jk}\Psi_{\rm tot})}{\partial r_{jk}} = -\frac{1}{a_s}. \tag{1}$$

Here, N denotes the total number of particles and $\vec{r}_j$ the position vector of the jth particle. No boundary conditions in the three- or higher-body sectors are needed, i.e., the Pauli exclusion principle "naturally" guarantees that the probability to find three or more particles on top of each other vanishes. The infinitely strongly interacting two-component Fermi gas is found to be mechanically stable and three-body losses are so low that the lifetime is large compared to the time scale associated with the Fermi energy and the other time scales of the system [6,7].

The situation for identical bosons is fundamentally different than that for two-component fermions. Unless the two-body boundary condition [see Eq. (1)], which is enforced for every pair, is supplemented by a three-body boundary condition (this can be achieved through a three-body potential or via a momentum cutoff, among others), the lowest energy of the Bose gas at unitarity is unbounded from below, i.e., the Bose gas undergoes a generalization of the Thomas collapse, which was first studied for three particles by Thomas in 1935 in the context of the triton [8]. The Thomas collapse is intimately related to the existence of an infinite tower of Efimov states for three identical bosons in free space [9–11] (no external confining potential).

When approaching the low-temperature unitary regime adiabatically, either by tuning the s-wave scattering length at low temperature or by decreasing the temperature at large s-wave scattering length [12–19], the system exhibits detrimental losses due to three-body recombination by which energetic atoms are being expelled from the trap. These three-body recombination processes are governed by Efimov physics [20–23]. Probing the gas at unitarity therefore requires jumping rapidly and nonadiabatically to this regime. Following nonadiabatic pathways, the unitary Bose gas—presumably in local but not in global equilibrium—has been probed experimentally using interferometric protocols [15,18]. The time-dependent contact at unitarity has been extracted and evidence that three-body Efimov states are being occupied during the nonadiabatic ramp sequence has been presented [13,18,19].

The theoretical treatment of the unitary Bose gas is highly nontrivial and a variety of approximate static and dynamic techniques have been applied [24–37], producing results that do not seem to yield a simple consistent physical picture. One line of work considers two- or three-body systems under external harmonic confinement [18,28,36]. Motivated by the physical insights that have already been gained from these two- and three-body studies, the present work considers the next larger system, namely the harmonically trapped four-body

system, for various positive two-body s-wave scattering lengths ranging from zero to infinity. The numerically obtained energy spectrum and the associated eigenstates are characterized.

The remainder of this paper is organized as follows. Section II introduces the system Hamiltonian and pertinent theoretical background. Sections III and IV present our results for the harmonically trapped three- and four-boson systems, respectively. Lastly, Sec. V presents a summary and an outlook.

II. SYSTEM HAMILTONIAN

We consider N identical bosons with mass m under spherically symmetric external confinement with angular frequency ω. The system Hamiltonian $H_{\rm tot}$,

$$H_{\rm tot} = H_{\rm c.m.} + H, \tag{2}$$

can be divided into the center-of-mass Hamiltonian $H_{\rm c.m.}$,

$$H_{\rm c.m.} = \frac{-\hbar^2}{2M}\nabla^2_{\vec{R}_{\rm c.m.}} + \frac{1}{2}M\omega^2\vec{R}^2_{\rm c.m.}, \tag{3}$$

and the relative Hamiltonian H,

$$H = \sum_{j=1}^{N-1}\left(\frac{-\hbar^2}{2\mu_j}\nabla^2_{\vec{\rho}_j} + \frac{1}{2}\mu_j\omega^2\vec{\rho}_j^{\,2}\right) + V_{\rm int}(\vec{\rho}_1,\ldots,\vec{\rho}_{N-1}). \tag{4}$$

Here, M denotes the total mass, $M = Nm$, and $\vec{R}_{\rm c.m.}$ the center-of-mass vector, $\vec{R}_{\rm c.m.} = N^{-1}(\vec{r}_1 + \cdots + \vec{r}_N)$, with $\vec{r}_j$ denoting the position vector of the jth particle measured with respect to the center of the trap. The relative Hamiltonian H is written in terms of the Jacobi vectors $\vec{\rho}_j$ and the associated Jacobi masses μ_j. For the purpose of this work, the explicit definition of the Jacobi coordinates is irrelevant. The important point is that the interaction potential $V_{\rm int}$ is independent of the center-of-mass vector $\vec{R}_{\rm c.m.}$. Correspondingly, the eigenstates $\Psi_{\rm tot}$ of $H_{\rm tot}$ separate into a center-of-mass piece $\Psi_{\rm c.m.}(\vec{R}_{\rm c.m.})$ and a relative piece $\Psi(\vec{\rho}_1,\ldots,\vec{\rho}_{N-1})$,

$$\Psi_{\rm tot}(\vec{r}_1,\ldots,\vec{r}_N) = \Psi_{\rm c.m.}(\vec{R}_{\rm c.m.})\Psi(\vec{\rho}_1,\ldots,\vec{\rho}_{N-1}). \tag{5}$$

Since the Schrödinger equation for the center-of-mass vector $\vec{R}_{\rm c.m.}$ is identical to that of a three-dimensional harmonic oscillator, the solutions can be written down readily. Our goal in this paper is to solve the relative Schrödinger equation

$$H\Psi(\vec{\rho}_1,\ldots,\vec{\rho}_{N-1}) = E\Psi(\vec{\rho}_1,\ldots,\vec{\rho}_{N-1}). \tag{6}$$

Realistic atom-atom interaction potentials support many two-body bound states. Consequently, the degenerate N-body gas (even the two-component Fermi gas) corresponds to a highly excited metastable state. To make the N-body problem tractable, we work with low-energy interactions that eliminate, from the outset, N-body states that correspond to deeply bound molecular clusters. It should be noted that this simplification also eliminates decay channels that are needed for three-body recombination processes, which are known to play a role in the quench experiments, to occur. In these experiments, the Bose gas disappears before global equilibrium is reached, restricting observations to systems that are in local equilibrium but not in global equilibrium. This work considers three different low-energy interactions.

A. Interaction model I

Model I assumes two-body hard-core interactions,

$$V^{\rm I}_{\rm int} = \sum_{j=1}^{N-1}\sum_{k>j}^{N} V^{\rm hc}_{\rm 2b}(r_{jk}), \tag{7}$$

where

$$V^{\rm hc}_{\rm 2b}(r_{jk}) = \begin{cases}\infty & \text{for} \quad r_{jk} \leqslant a_s,\\ 0 & \text{for} \quad r_{jk} > a_s.\end{cases} \tag{8}$$

This model interaction, which has been used extensively in the literature (see, e.g., Refs. [38–40]), is expected to provide a reliable description of the weakly repulsive Bose gas. Since the range of the hard-core potential increases with increasing a_s, this interaction yields model-dependent results when $a_s/a_{\rm ho}$ is not small. The ground state of the time-independent N-particle Schrödinger equation for this model interaction can be found efficiently using the diffusion quantum Monte Carlo technique [40,41]. For positive and sufficiently small a_s (see Secs. III and IV for more quantitative statements), this ground state corresponds to the gaslike state that we are interested in. No excited states are considered for model I.

B. Interaction model II

Model II assumes an attractive two-body Gaussian interaction $V^{\rm G}_{\rm 2b}(r_{jk})$ with depth v_0 ($v_0 < 0$) and range r_0,

$$V^{\rm G}_{\rm 2b}(r_{jk}) = v_0\exp\left[-\left(\frac{r_{jk}}{\sqrt{2}r_0}\right)^2\right]. \tag{9}$$

Throughout this work, the range is fixed at $r_0 = 0.025a_{\rm ho}$ and the depth v_0 is adjusted to dial in the desired s-wave scattering length a_s ($a_s \geqslant 0$). We only consider depths for which the Gaussian potential supports one two-body s-wave bound state in free space (at unitarity, this bound state has zero energy). To prevent the formation of deeply bound molecular three- and four-body states, a repulsive three-body Gaussian potential $V^{\rm G}_{\rm 3b}(r_{jkl})$ with height V_0 and range R_0 is added,

$$V^{\rm G}_{\rm 3b}(r_{jkl}) = V_0\exp\left[-\left(\frac{r_{jkl}}{\sqrt{2}R_0}\right)^2\right]. \tag{10}$$

Here, r_{jkl} denotes the "triple subhyperradius,"

$$r_{jkl} = \sqrt{r^2_{jk} + r^2_{jl} + r^2_{kl}}. \tag{11}$$

For the $N = 3$ system, there exists one such triple subhyperradius, which coincides with the N-body hyperradius R,

$$R = \sqrt{\sum_{j=1}^{N-1}\sum_{k>j}^{N} r^2_{jk}}. \tag{12}$$

For the $N = 4$ system, there exist four triple subhyperradii. Throughout, we fix R_0 at $\sqrt{8}r_0 \approx 0.071a_{\rm ho}$. The height V_0 is varied to investigate the dependence of the results on the three-body potential. Putting things together, interaction model II reads

$$V^{\rm II}_{\rm int} = \sum_{j=1}^{N-1}\sum_{k>j}^{N} V^{\rm G}_{\rm 2b}(r_{jk}) + \sum_{j=1}^{N-2}\sum_{k>j}^{N-1}\sum_{l>k}^{N} V^{\rm G}_{\rm 3b}(r_{jkl}). \tag{13}$$

While the repulsive three-body Gaussian potential eliminates deep-lying molecular states, the resulting Hamiltonian supports states with gaslike and molecularlike character (see Secs. III and IV for details). To obtain the entire low-energy spectrum and to subsequently analyze what the characteristics of the eigenstates are, we employ a basis set expansion approach. The eigenstates Ψ are expanded in terms of a set of nonorthogonal explicitly correlated Gaussian basis functions, which depend on the interparticle distance coordinates and a set of nonlinear variational parameters [42,43]. The nonlinear variational parameters, which are optimized semistochastically, give the flexibility to describe correlations at different length scales, namely, at the scales of the range of the interaction potential and the harmonic-oscillator length. The resulting generalized eigenvalue problem is solved through diagonalization [42,43]. The resulting eigenvalues are, according to Ritz' variational principle, variational upper bounds to the true eigenenergies (this statement holds for the ground and the excited states) [42]. Throughout this paper, only states Ψ with vanishing relative orbital angular momentum L and positive parity Π are considered. These states constitute a small subset of the entire set of eigenstates.

As the two-body depth v_0 becomes more negative, the four-body system supports an increasing number of states with negative energy. As a consequence, the lowest BEC state (see below for a definition) is a fairly highly excited state of the Hamiltonian with interaction model II. For v_0 not too negative, we optimize one eigenstate at a time. We follow the same general strategy as the one that was pursued to determine a large number of eigenenergies and eigenstates of the two-component four-particle Fermi gas [44]. The basis set that describes, e.g., the tenth eigenstate accurately may describe the nine energetically lower-lying states comparatively poorly. However, as long as the basis captures the nine lower-lying states, even if poorly, the energy of the tenth state provides an upper variational bound for the tenth state. A typical basis set consists of 600 (for low state numbers) to 2000 (for large state numbers) fully symmetrized basis functions.

The portion of the four-body spectrum that we are interested in consists of more and more highly excited states as the s-wave scattering length decreases (i.e., as v_0 becomes more negative). As a consequence, it becomes increasingly tedious to generate a basis set for each eigenstate. In particular, even if we do not optimize each state, to obtain a tight bound for the energy of, say, state number 70, we still need to describe 69 lower-lying states. As an alternative, we employ a "target state approach," which optimizes the state whose energy is greater than but closest to a preset target energy. The target state approach is similar in spirit to what has been used to identify resonance states (see, e.g., Ref. [45]). For example, if we expect that the system supports a state with energy E^*, then we set the target energy to $E^* - \Delta E$, where ΔE is positive and of the order of a tenth of $E_{\rm ho}$. When we enlarge the basis set, we add basis functions that lower the energy of the state whose energy is above the target energy and closest to it. As more basis functions are added, the energy of this state drops below $E^* - \Delta E$ and we optimize the state with the next larger energy. When plotting the eigenenergies as a function of the inverse of the number of basis functions, we observe convergence of the energy corresponding to different state numbers. If we repeat the calculation for different ΔE and find the same final energy, then we can be fairly sure that we have found an isolated eigenenergy, i.e., the energy of an eigenstate away from avoided crossings. Since we do not, in this case, describe all the lower-lying states, the resulting energy, extrapolated to the infinite basis set limit, does not provide a strict variational upper bound. The advantage of this approach is that the majority of the basis functions added is used to improve the description of the state of interest without having to describe (even if relatively poorly) all the lower-lying states.

C. Interaction model III

Model III employs two-body zero-range interactions. As already alluded to in the Introduction, the two-body interactions can be accounted for by enforcing the boundary condition in Eq. (1) on the relative many-body eigenstate Ψ. Much of the remainder of this subsection focuses on unitarity.

At unitarity, the noninteracting Hamiltonian with the boundary condition given in Eq. (1) supports relative eigenstates that can be written as a direct product of a function $\Phi_{\nu q}$ that depends on the four-body hyperradius R and a function ϕ_ν that is independent of R [4,46,47],

$$\Psi_{\nu q}(\vec{\rho}_1,\ldots,\vec{\rho}_{N-1}) = R^{-(3N-4)/2}\Phi_{\nu q}(R)\phi_\nu(\vec{\Omega}). \quad (14)$$

Here, $\vec{\Omega}$ collectively denotes the $3N-4$ hyperangular coordinates (the definition of the hyperangles is not important for the discussion that follows). The eigenenergies corresponding to these eigenstates are given by

$$E^{\rm unit}_{\nu q} = (2q + s_\nu + 1)E_{\rm ho}, \quad (15)$$

where $q = 0,1,\ldots$ denotes the hyperradial quantum number and s_ν (which is real valued) would be obtained by solving a differential equation in the hyperangular degrees of freedom. The harmonic-oscillator energy $E_{\rm ho}$ is defined through $E_{\rm ho} = \hbar\omega$. The quantum number ν enumerates the solutions of the differential equation in the hyperangular coordinates. Equation (15) is a consequence of the fact that each hyperradial potential curve, which is characterized by s_ν, supports a ladder of states with energy spacing $2E_{\rm ho}$; this spacing is the same as for the noninteracting system (the s_ν values are, however, in general different) [4]. The values of s_ν for the unitary Bose gas are, for $N > 3$, challenging to determine and, to the best of our knowledge, not known. For $N = 3$, the s_ν values can be determined semianalytically with arbitrary accuracy [10,48,49]. We refer to the states of the form given in Eq. (14) with eigenenergies of the form given in Eq. (15) as universal states. Universal in this sense implies that the eigenenergies and eigenstates are indifferent to the three-body potential, and are thus characterized by the two-body s-wave scattering length alone.

Importantly, model III supports a second class of states at unitarity that we refer to as nonuniversal (for $N = 3$, Ref. [50] refers to this class of states as Efimovian). To introduce these nonuniversal states, we consider the $N = 3$ system. The hyperangular equation for $N = 3$, which is solved subject to the two-body boundary condition, yields one imaginary eigenvalue, namely $s_0 = \imath 1.00624\ldots$. Neglecting for the moment the external confinement, this eigenvalue gives rise to

a purely attractive effective hyperradial potential curve that is proportional to $-(|s_0|^2 + 1/4)R^{-2}$ and supports an infinite number of three-body bound states, with the ratio between neighboring energy levels being equal to $\exp(\pi/|s_0|)^{-2} \approx 1/515$. To fix the absolute position of the energy levels, a small-R boundary condition on the hyperradial function Φ_0 needs to be specified [9–11]. Such an additional boundary condition is not needed for the universal states, since the probability to find three bosons at the same location is vanishingly small "on its own" due to the repulsive small-R behavior of the effective hyperradial potential curves for real s_ν (if an additional small-R boundary condition was added, the universal states would be insensitive to it). If the trap is added, the spacing between the energy of consecutive nonuniversal states is modified drastically. The resulting energy spacings depend on q and differ, in general, from the $2E_{\rm ho}$ spacing that is a key signature of the universal states [50,51].

The nonuniversal states of the trapped $N = 4$ unitary system have not yet been studied in much depth [52,53]. When solving the hyperangular equation for $N = 4$, the three-body boundary condition for each triple should be accounted for in addition to the two-body boundary condition for each pair. While this hyperangular equation has not yet been solved for zero-range interactions, it has been solved for finite-range interactions [54]. The fixed-R hyperangular eigenvalues were shown to depend on the four-body hyperradius R, implying nonseparability of the hyperradial and hyperangular degrees of freedom. Setting ω to zero, there exist as many effective hyperradial potential curves as there exist three-body Efimov states and the large-R values (R can be very large) of these potential curves are just the energies of the three-body Efimov states [54]. This is distinctly different from the three-boson system, which supports one effective hyperradial potential curve at unitarity in which an infinity of nonuniversal three-body states live (the other potential curves support universal states).

The confining potential "cuts off" the asymptotic region for all but the few lowest effective free-space hyperradial four-body potential curves (depending on the system parameters, it might be all but one). The term "cuts off" is used here to indicate that the asymptotic behavior of the effective potential curves is suppressed by the quadratically increasing confining potential, which forces the wave function to fall off at much smaller R than it would in the absence of the trap, where there exist two four-body states that are tied to each Efimov trimer [54,55]. To determine the eigenenergies of the nonuniversal states, the coupling (which may be small) between different potential curves needs to be accounted for even at unitarity; this is, again, distinctly different from the three-boson system where the coupling at unitarity vanishes for the universal *and* the nonuniversal states. It is expected that the resulting energy ladders for the nonuniversal states of the trapped four-boson system are characterized by energy spacings that, in general, differ from $2E_{\rm ho}$.

The four-body results at unitarity presented in Sec. IV are not obtained by first solving the hyperangular differential equation and by then subsequently solving a set of coupled differential equations in the hyperradius. Instead, the four-body results are obtained by treating all relative degrees of freedom on equal footing. The resulting energy spectrum and eigenfunctions are, however, analyzed within the hyperspherical coordinate framework introduced above. A main outcome of the analysis for $N = 4$ will be that some states do not fit neatly into the categories of universal or nonuniversal. We will denote these states as quasiuniversal. To illustrate aspects of our approach, the next section presents three-body results for interaction models I, II, and III.

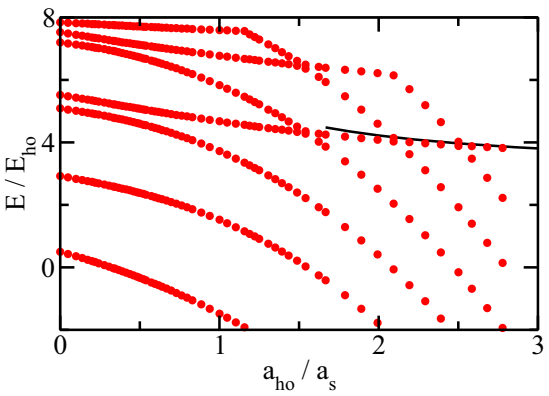

FIG. 1. Energy spectrum for three harmonically trapped identical bosons as a function of $a_{\rm ho}/a_s$. Circles show the relative energy of the seven energetically lowest-lying states with $L^\Pi = 0^+$ symmetry for model II with $V_0 = 97\,700E_{\rm ho}$. The solid line shows the relative energy of the lowest state for two-body hard-core interactions (model I).

Moving from unitarity to finite s-wave scattering lengths, the eigenstates of the harmonically trapped N-boson system cannot *a priori* be divided into universal and nonuniversal states even in principle. Separability between the hyperangular and hyperradial degrees of freedom does generally not exist and the energy spectrum is expected to exhibit series of avoided crossings. The next section illustrates that one can, away from the avoided crossings, nevertheless meaningfully categorize states as universal and nonuniversal.

III. $N = 3$ SYSTEM

To set the stage for our $N = 4$ results, this section summarizes selected results for the $N = 3$ system. Circles in Fig. 1 show the relative three-body spectrum for the interaction model II as a function of the inverse of the s-wave scattering length for a fixed three-body interaction; specifically, V_0 is set to $97\,700E_{\rm ho}$. At unitarity, the (ν,q) quantum numbers (see Table I) are assigned as follows. Using the two smallest real s_ν ($s_1 = 4.46529\ldots$ and $s_2 = 6.81836\ldots$) for the zero-range model in Eq. (15), the following relative zero-range energies at unitarity are found: $E^{\rm unit}_{1,0} = 5.46529E_{\rm ho}$, $E^{\rm unit}_{1,1} = 7.46529E_{\rm ho}$, and $E^{\rm unit}_{2,0} = 7.81836E_{\rm ho}$ [50]. These zero-range energies for the universal states agree well with a subset of our numerical energies for model II: $E = 5.5187E_{\rm ho}$, $7.5258E_{\rm ho}$, and $7.8452E_{\rm ho}$. The differences, which are of the order of 1%, are attributed to the fact that the range of our two-body Gaussian potential is $r_0 = 0.025a_{\rm ho}$ and not zero. The hyperradial densities $P(R)$, obtained for model II, confirm this assignment. For example, the hyperradial density for a state with quantum number q has $q - 1$ zeros along the hyperradial coordinate.

TABLE I. Three-boson properties at unitarity for model II with $V_0 = 97\,700 E_{\rm ho}$. Column 1 lists the state number. Column 2 reports the relative energy. Columns 3 and 4 report the ν and q quantum numbers. Columns 5 and 6 report the two- and three-body contacts C_2 and C_3, respectively. Column 7 lists the square of the overlap for the states at unitarity with an eigenstate of model II with $v_0 = 0$ and $V_0 = 97\,700 E_{\rm ho}$. The occupation probabilities for the states listed add up to 0.964. Column 8 indicates whether the state is universal or nonuniversal. The energies are estimated to be converged to $0.0010 E_{\rm ho}$ or better.

State no.	$E/E_{\rm ho}$	ν	q	$C_2 a_{\rm ho}$	$C_3 a_{\rm ho}^2$	Probability	Comment
1	0.5000	0	0	35.6	0.478	0.412	Nonuniversal
2	2.9217	0	1	22.4	0.334	0.426	Nonuniversal
3	5.0895	0	2	18.8	0.323	2×10^{-4}	Nonuniversal
4	5.5187	1	0	21.6	9×10^{-6}	0.096	Universal
5	7.2005	0	3	17.3	0.326	1×10^{-4}	Nonuniversal
6	7.5258	1	1	20.5	3×10^{-5}	0.027	Universal
7	7.8452	2	0	7.15	2×10^{-7}	0.003	Universal
8	9.2874	0	4	15.4	0.336	5×10^{-5}	Nonuniversal

The remaining energies at unitarity (see Table I) are identified as belonging to nonuniversal states, i.e., to states that are supported by the effective hyperradial potential curve labeled by $\nu = 0$ (imaginary s_0). The corresponding energy spacings ($2.4217 E_{\rm ho}$, $2.1678 E_{\rm ho}$, $2.1110 E_{\rm ho}$, and $2.0869 E_{\rm ho}$) deviate notably from $2E_{\rm ho}$; the deviations decrease with increasing q. In the absence of the harmonic trap, the lowest relative three-body energy is $E_{\rm fs} = -1.19\times10^{-4}\hbar^2/(m r_0^2)$. Using this to estimate the size $L_{\rm fs}$ of the free-space trimer at unitarity via the expression $L_{\rm fs} = (\kappa_{\rm fs}^*)^{-1}$, where the binding momentum $\kappa_{\rm fs}$ is defined through $\kappa_{\rm fs} = \sqrt{m|E_{\rm fs}|/\hbar^2}$ and $\kappa_{\rm fs}^*$ denotes the binding momentum at unitarity, we find $L_{\rm fs} = 91.5 r_0$ or, using $r_0 = 0.025 a_{\rm ho}$, $L_{\rm fs} = 2.29 a_{\rm ho}$, i.e., the lowest free-space Efimov trimer is roughly of the same size as the harmonic-oscillator length of the external confinement. If we use the lowest relative three-body energy for the finite-range model II of the trapped three-boson system (namely $E = 0.5000 E_{\rm ho}$) as input for the zero-range model III [this can be viewed as setting the small-R boundary condition; see Eqs. (11)–(13) of Ref. [50]], the resulting nonuniversal relative energies for model III ($2.9019 E_{\rm ho}$, $5.0587 E_{\rm ho}$, $7.1597 E_{\rm ho}$, and $9.2351 E_{\rm ho}$) agree reasonably well with those obtained for model II (see Table I). The deviations of around 1% are attributed to the finite r_0 and R_0 values of the two- and three-body potentials. The above analysis shows that model II provides three-body energies at unitarity that are close to those for model III.

In addition to the energies, we calculate the two- and three-body contacts C_2 and C_3 [56],

$$C_2 = -\frac{8\pi m}{\hbar^2}\frac{\partial E}{\partial\left(a_s^{-1}\right)} \tag{16}$$

and

$$C_3 = -\frac{m\kappa_{\rm fs}}{2\hbar^2}\frac{\partial E}{\partial \kappa_{\rm fs}}. \tag{17}$$

In practice, the derivative on the right-hand side of Eq. (16) is calculated by changing v_0 while keeping V_0 constant and using finite differencing. Changing v_0 translates into a change of the free-space two-body scattering length a_s. The derivative on the right-hand side of Eq. (17), in turn, is calculated by changing V_0 while keeping v_0 constant. Changing V_0 translates into a change of the lowest relative free-space three-body energy $E_{\rm fs}$ and thus of the corresponding binding momentum $\kappa_{\rm fs}$. Columns 5 and 6 of Table I show the two- and three-body contacts for the harmonically trapped three-boson system at unitarity. The universal states are characterized by an extremely small C_3 (C_3 should be zero for model III) since the likelihood of finding three bosons in close vicinity to each other is zero for this class of states. The normalization of the three-body contact C_3 in Eq. (17) is chosen such that $C_3 = (\kappa_{\rm fs}^*)^2$ for a free-space Efimov trimer at unitarity described by model III. For model II with $V_0 = 97{,}700 E_{\rm ho}$, the three-body contact for the lowest free-space Efimov trimer is, converted to trap units (using $r_0 = 0.025 a_{\rm ho}$), equal to $0.437(a_{\rm ho})^{-2}$. Table I shows that the addition of the external confinement leads to a slight increase of C_3 for the $(\nu,q) = (0,0)$ state [$C_3 = 0.478(a_{\rm ho})^{-2}$]. This makes sense intuitively since the trap forces the free-space Efimov trimer into a "smaller space." The two-body contact C_2 is roughly comparable for the universal and nonuniversal states.

Next, we look at how the energy levels evolve as we go from infinite to finite to vanishingly small positive s-wave scattering lengths (see Refs. [51,57] for early studies). The energy of all the states shown in Fig. 1 decreases with increasing $a_{\rm ho}/a_s$, as the two-body potential becomes deeper. The state with relative energy $5.5187 E_{\rm ho}$ at unitarity, i.e., the lowest universal state, goes through a sequence of fairly narrow avoided crossings and approaches, on the scale of Fig. 1, the relative energy for the hard-core interaction model around $a_{\rm ho}/a_s = 2$ (solid line in Fig. 1). If we prepare the three-boson system in the noninteracting state (which is universal) and then adiabatically increase the s-wave scattering length, the system will—neglecting the avoided crossings (they could be jumped across)—end up in the lowest universal state at unitarity. In this sense, we identify this state as representing the "BEC state," all the way to unitarity.

Alternatively, we may consider preparing the three-boson system in the lowest noninteracting state and then instantaneously jumping the scattering length to infinity. In this scenario, the occupation probability of each of the states at unitarity is given by the square of the overlap between the initial state and the respective state at unitarity (see also Ref. [28]). Table I shows the occupation probabilities for an initial state that does not "feel" a two-body potential (v_0 is set to zero) but does "feel" the three-body Gaussian potential. The relative energy of this state is very close to that of the noninteracting state ($3.0004 E_{\rm ho}$ compared to $3E_{\rm ho}$). The considered quench leads predominantly to the occupation of nonuniversal states. Roughly speaking, the states at unitarity that have an energy that is comparable to the energy of the initial state have the largest occupation probabilities. This observation is consistent with the discussion presented in Ref. [28]. While the occupation probabilities of the nonuniversal states depend on the three-body parameter, those of the universal states are to a very good approximation independent of the height V_0 of the repulsive three-body Gaussian potential.

To investigate the dependence of the three-body energies on the height V_0 of the repulsive three-body Gaussian potential

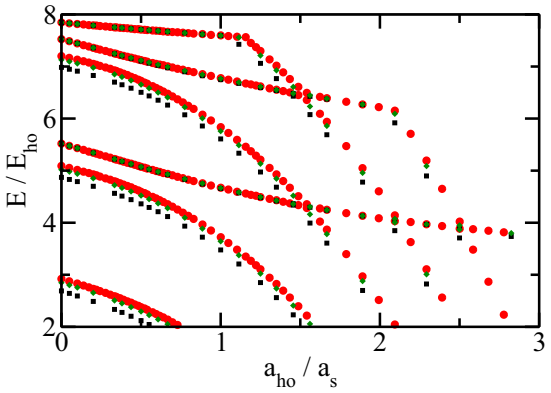

FIG. 2. Dependence of the energy spectrum for three identical harmonically trapped bosons on the height V_0 of the three-body Gaussian potential. The circles, diamonds, and squares show the relative energy as a function of $a_{\rm ho}/a_s$ for $V_0 = 97\,700 E_{\rm ho}$ (same as in Fig. 1), $V_0 = 40\,000 E_{\rm ho}$, and $V_0 = 10\,000 E_{\rm ho}$, respectively. Only states with $L^\Pi = 0^+$ symmetry are considered.

explicitly over the entire scattering length regime, we calculate the three-body spectrum for two other V_0 values, namely $V_0 = 10\,000 E_{\rm ho}$ and $40\,000 E_{\rm ho}$. The resulting energies are shown by squares and diamonds in Fig. 2 together with the energies for $V_0 = 97\,700 E_{\rm ho}$ (circles). Away from the avoided crossings, the states follow one of two behaviors: the energies are to a good approximation independent of V_0 or the energies display an appreciable dependence on V_0. This provides a means to classify the states, away from the avoided crossings, as universal and nonuniversal not only at unitarity but also for finite scattering lengths.

IV. $N = 4$ SYSTEM

This section summarizes our results for the harmonically trapped four-boson system. Circles in Fig. 3 show the $L^\Pi = 0^+$ energy spectrum for model II with the height of the repulsive Gaussian potential set to $V_0 = 97\,700 E_{\rm ho}$ (this is the same V_0 as that used in Fig. 1) as a function of $a_{\rm ho}/a_s$. At first glance, the energy spectrum, with its many avoided crossings (a blowup is shown in Fig. 4), looks quite "messy." The four-boson Hamiltonian supports many energy levels that are positive for infinite scattering length and go, sometimes after passing through multiple avoided crossings, to negative energies as $a_{\rm ho}/a_s$ increases, i.e., as the two-body potential becomes deeper. Based on the $N = 3$ analysis presented in the previous section, we expect that these rapidly falling four-body levels correspond to nonuniversal states. The four-boson Hamiltonian also supports a few energy levels that change less with increasing $a_{\rm ho}/a_s$ and remain positive for the largest $a_{\rm ho}/a_s$ (smallest s-wave scattering lengths) considered. The lowest of these energy levels plays, as will be shown below, a role similar to the lowest universal state of the three-boson system.

We start our discussion by analyzing the unitary regime. The energies of the lowest 26 states at unitarity are listed in column 2 of Table II. To assign the (approximate) hyperangular and hyperradial quantum numbers ν and q (see columns 3 and 4 of Table II), we followed—inspired by the discussion

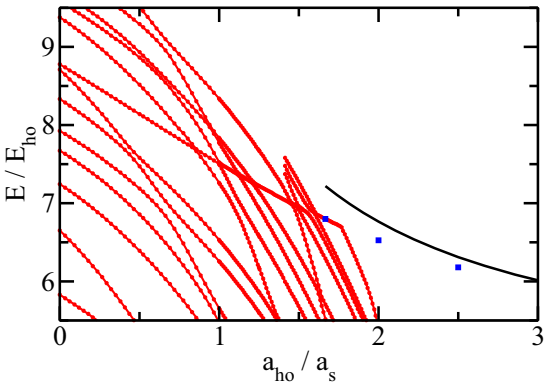

FIG. 3. Energy spectrum for four harmonically trapped identical bosons as a function of $a_{\rm ho}/a_s$. Only states with $L^\Pi = 0^+$ symmetry are considered. The filled circles (neighboring points are connected by solid lines) show the relative energies for model II with $V_0 = 97\,700 E_{\rm ho}$. The number of states considered is larger for $a_{\rm ho}/a_s \gtrsim 1.4$ than for $a_{\rm ho}/a_s \lesssim 1.4$. The squares show the relative energies for model II with $V_0 = 97\,700 E_{\rm ho}$ obtained using the "target state approach" [these energies are not necessarily upper bounds; moreover, the error bar (not shown) for $a_{\rm ho}/a_s = 2.5$ is comparatively large]. For comparison, the solid line shows the relative ground-state energy for two-body hard-core interactions (model I).

presented in Sec. III—a multistep process. Note that the quantum number ν represents an index that counts the different presumed hyperspherical potential curves. In a more complete analysis one might hope to identify a set of quantum numbers for the multiple hyperangular degrees of freedom.

First, we vary V_0 while keeping the two-body potential fixed. Energy levels that do not move when V_0 is changed over a reasonable range are identified as universal; for these states, the three-body contact C_3 for model II with $V_0 = 97\,700 E_{\rm ho}$ is equal to $0.004(a_{\rm ho})^{-2}$ or smaller (see column 5 of Table II). Energy levels that do move when V_0 is changed are identified as nonuniversal; for these states, the three-body contact C_3 for model II with $V_0 = 97\,700 E_{\rm ho}$ lies between $0.045(a_{\rm ho})^{-2}$ and $1.35(a_{\rm ho})^{-2}$. Interestingly, the majority of the low-lying states is nonuniversal.

In the absence of the external confinement, the $(\nu,q) = (0,0)$ state is tied to the lowest free-space Efimov trimer. For $V_0 = 97\,700 E_{\rm ho}$, the energy ratio between the $N = 4$ and

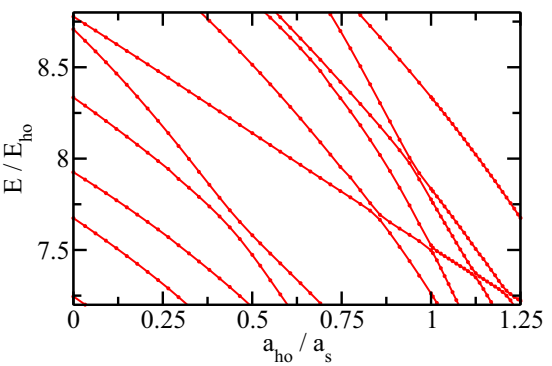

FIG. 4. Blowup of a portion of the energy spectrum shown in Fig. 3. It can be seen that the avoided crossings are quite narrow.

TABLE II. Four-boson properties at unitarity for model II with $V_0 = 97\,700 E_{\rm ho}$. Column 1 lists the state number. Column 2 reports the relative energy E. Columns 3 and 4 report the ν and q quantum numbers. Columns 5 and 6 list the two- and three-body contacts C_2 and C_3, respectively. Column 7 lists the square of the overlap for the states at unitarity with an eigenstate of model II with $v_0 = 0$ and $V_0 = 97\,700 E_{\rm ho}$. The occupation probabilities for the states listed add up to 0.952. Column 8 indicates whether the state is universal, quasiuniversal, or strongly nonuniversal.

State no.	$E/E_{\rm ho}$	ν	q	$C_2 a_{\rm ho}$	$C_3 a_{\rm ho}^2$	Probability	Comment
1	−0.0622	0	0	55.0	1.35	0.224	Strongly nonuniversal
2	2.7139	0	1	39.6	0.895	0.455	Strongly nonuniversal
3	4.5646	1	0	54.2	0.318	0.008	Strongly nonuniversal
4	5.0460	0	2	35.9	0.785	0.016	Strongly nonuniversal
5	5.8297	2	0	33.7	0.384	0.160	Strongly nonuniversal
6	6.6516	1	1	51.1	0.295	0.003	Strongly nonuniversal
7	7.2457	0	3	34.6	0.744	1×10^{-4}	Strongly nonuniversal
8	7.6741	3	0	33.3	0.200	0.002	Strongly nonuniversal
9	7.9257	2	1	31.1	0.367	0.015	Strongly nonuniversal
10	8.3345	4	0	34.8	2×10^{-4}	0.017	Universal
11	8.7082	1	2	48.6	0.278	4×10^{-4}	Strongly nonuniversal
12	8.7773	5	0	31.3	0.095	0.020	Quasiuniversal
13	9.3789	0	4	35.0	0.694	5×10^{-4}	Strongly nonuniversal
14	9.5758	6	0	30.0	0.206	0.003	Strongly nonuniversal
15	9.7113	3	1	31.7	0.214	7×10^{-6}	Strongly nonuniversal
16	9.9968	2	2	29.3	0.370	0.004	Strongly nonuniversal
17	10.3381	4	1	33.9	3×10^{-4}	0.007	Universal
18	10.4857	7	0	19.0	0.061	3×10^{-4}	Quasiuniversal
19	10.5462	8	0	16.0	0.045	0.001	Quasiuniversal
20	10.7616	1	3	45.6	0.258	7×10^{-5}	Strongly nonuniversal
21	10.7895	5	1	30.3	0.099	0.009	Quasiuniversal
22	10.8732	9	0	22.9	0.106	0.001	Quasiuniversal
23	11.2272	10	0	16.2	0.004	0.001	Universal
24	11.4668	0	5	35.8	0.562	9×10^{-4}	Strongly nonuniversal
25	11.6047	6	1	27.9	0.321	0.001	Strongly nonuniversal
26	11.7560	3	2	30.1	0.235	1×10^{-4}	Strongly nonuniversal

$N = 3$ free-space energies is 4.59, which is quite close to the zero-range value of 4.6108 [58]. The three-body contact of the trapped four-boson states in the $\nu = 0$ family is comparatively large [larger than $0.562(a_{\rm ho})^{-2}$ for the states listed in Table II]. The three-body contact for the $(\nu,q) = (0,0)$ state is $1.35(a_{\rm ho})^{-2}$, which is close to the three-body contact for the lowest free-space tetramer [the three-body contact of the lowest free-space tetramer for $V_0 = 97\,700 E_{\rm ho}$ is equal to $1.37(a_{\rm ho})^{-2}$].

The three-body contacts of the other nonuniversal states fall, roughly, into two categories: either C_3 is around $0.3(a_{\rm ho})^{-2}$ (this is similar to the three-body contacts of the nonuniversal $N = 3$ states [excluding the $(\nu,q) = (0,0)$ state]); or C_3 is less than about $0.1(a_{\rm ho})^{-2}$. We refer to states with C_3 less than about $0.1(a_{\rm ho})^{-2}$ as "quasiuniversal" (these states display a comparatively weak dependence on $\kappa_{\rm fs}$) and to states with C_3 greater than about $0.1(a_{\rm ho})^{-2}$ as "strongly nonuniversal" (these states display a comparatively strong dependence on $\kappa_{\rm fs}$); see column 8 of Table II. While this classification scheme is somewhat arbitrary, we employ it since it provides a means to categorize the sensitivity of the trapped $N = 4$ states on the three-body parameter or, equivalently, the three-body potential. Within each ν family, the three- and two-body contacts decrease or remain (roughly) the same with increasing q; the small increase in selected cases might be due to numerical inaccuracies or might indicate small irregularities on top of the overall pattern.

As a second step in the classification of states, we consider the spacings of the energies. The energy spacings between consecutive universal states that live in the same effective hyperradial potential curve should be equal to $2E_{\rm ho}$. Table II shows that the spacing between the energies labeled by $(\nu,q) = (4,0)$ and $(4,1)$ is very close to $2E_{\rm ho}$. The small deviation of $0.004E_{\rm ho}$ may be due to numerical inaccuracies or due to the use of the two-body Gaussian potential with finite r_0 instead of the two-body zero-range Fermi-Huang pseudopotential.

In addition, we analyze the hyperradial density $P(R)$, which is normalized such that $\int_0^\infty P(R)dR = 1$. The value of the hyperradial density $P(R)$ tells one the likelihood to find the four-boson system at the hyperradius R. Figure 5(e) shows the hyperradial densities for the states labeled by $(\nu,q) = (4,0)$ and $(4,1)$. The hyperradial density for the $q = 1$ states goes to zero at about $R = 5.8a_{\rm ho}$, indicating that the corresponding eigenstate can be written, at least to a very good approximation, as a product state [see Eq. (14)] even though we are using finite-range interactions. The finite ranges r_0 and R_0 of our two- and three-body potentials could, in principle, introduce a small violation of the separability. For the analysis in this paper, this effect is, however, negligible. This nearly complete factorization further supports the idea of these $\nu = 4$ states

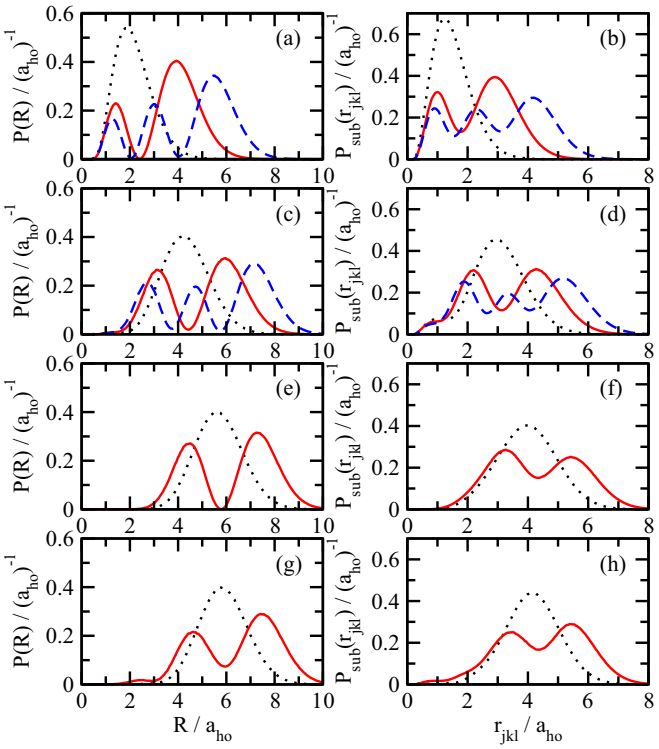

FIG. 5. Structural properties of the harmonically trapped four-boson system at unitarity for interaction model II with $V_0 = 97\,700 E_{\rm ho}$. The hyperradial density $P(R)$ (left column) and subhyperradial density $P_{\rm sub}(r_{jkl})$ (right column) are shown for different ν families (the first, second, third, and fourth row are for $\nu = 0$, $\nu = 1$, $\nu = 4$, and $\nu = 5$, respectively). The density of the lowest state ($q = 0$) in a given family is shown by a dotted line, that of the second-lowest state ($q = 1$) in a given family by a solid line, and that of the third-lowest state ($q = 2$) in a given family by a dashed line.

being universal, and clarifies the assignment of the quantum numbers $q = 0$ and 1.

For the nonuniversal states, the assignment of the (ν,q) quantum numbers is not quite as straightforward. A key difference between the $N = 3$ and $N = 4$ systems is that the nonuniversal states of the $N = 4$ system do not necessarily separate into a hyperradial piece and a hyperangular piece (see Sec. II). One consequence is that the (ν,q) quantum numbers assigned to the nonuniversal $N = 4$ states are approximate and not exact quantum numbers. A closely related consequence is that the hyperradial densities of the nonuniversal $N = 4$ states do not necessarily vanish for states with $q > 0$. The position of the hyperradial nodes can depend nontrivially on the hyperangles, implying that $P(R)$ shows "washed out" zeros. Figures 5(c) and 5(g) show examples of this for the $\nu = 1$ and 5 families, respectively. For these families, the hyperradial densities for $q > 0$ show minima that have finite and not vanishing amplitude. Figures 5(a) ($\nu = 0$ family), 5(c) ($\nu = 1$ family), 5(e) ($\nu = 4$ family), and 5(g) ($\nu = 5$ family) also show that the hyperradial densities of states that live, approximately, in the same effective hyperradial potential curve (labeled by ν) exhibit similar behavior at small R. This observation lends further support for our assignment of the quantum numbers.

The energy-level spacings $E_{\nu,q+1} - E_{\nu,q}$ between neighboring nonuniversal states is expected to change (roughly) monotonically from being larger than $2E_{\rm ho}$ for $q = 0$ to approximately $2E_{\rm ho}$ for large q. Inspection of Table II shows that our assignment of the quantum numbers is consistent with this expectation.

To shed further light on the structural properties of the trapped four-boson system at unitarity, we take a closer look at Fig. 5. Selected aspects of the hyperradial densities $P(R)$ (left column) were already discussed above. Comparing the hyperradial densities for $\nu = 0$, 1, 4, and 5 [Figs. 5(a), 5(c), 5(e), and 5(g)], it can be seen that the $P(R)$ for $\nu = 0$ (the $q = 0$ state approaches the lowest four-boson state that is linked to the free-space Efimov trimer when the trap is removed) has a nonvanishing amplitude at much smaller R than the states with higher ν. Moreover, the $\nu = 4$ states (these are universal states) have essentially vanishing amplitude at $R \lesssim 2a_{\rm ho}$. The $(\nu,q) = (5,0)$ state, which is quasiuniversal and identified below as the BEC state, displays a small "bump" at small R, which we interpret as a signature of the weak dependence on the three-body potential. Figures 5(b), 5(d), 5(f), and 5(h) show the subhyperradial density $P_{\rm sub}(r_{jkl})$, which corresponds to the probability of finding three of the four bosons at a particular subhyperradius r_{jkl}. The strongly nonuniversal $\nu = 0$ and $\nu = 1$ states [Figs. 5(b) and 5(d)] display an appreciable amplitude in the $r_{jkl} \lesssim a_{\rm ho}$ region. By comparison, the amplitude of the quasiuniversal $\nu = 5$ states [Fig. 5(h)] is, in the same region, notably smaller and that of the universal $\nu = 4$ states [Fig. 5(f)] is essentially zero.

As an aside, we note that the two-body contact C_2 at unitarity for model II with $V_0 = 97\,700 E_{\rm ho}$ (see column 5 of Table II) varies by less than a factor of 4. This is in contrast to the three-body contact, which varies over roughly four orders of magnitude. Generally speaking, the two-body contact for the trapped $N = 4$ system is larger than that for the trapped $N = 3$ system. This makes sense intuitively since the four-body system contains twice as many pairs as the three-body system (six pairs compared to three pairs). While the two-body contact C_2 is obtained by looking at the variation of the energy with $(a_s)^{-1}$, it also tells one the likelihood of finding two bosons in close proximity from each other. The fact that the two-body contact is of comparable magnitude for the universal and nonuniversal states is, at least in part, a consequence of the fact that the two-body boundary condition is enforced for both classes of states and that Table II is limited to the low-energy portion of the $L^\Pi = 0^+$ spectrum. We expect the two-body contact to be notably smaller for a subset of the high-lying states and for states with finite orbital angular momentum.

As discussed above, the four-boson spectrum depends on the two-body s-wave scattering length (or, alternatively, the lowest relative energy of the trapped two-boson system) and, in our model II, the height of the three-body repulsive Gaussian. The latter can, as done when calculating the three-body contact, be converted to the free-space $\kappa_{\rm fs}^*$ (three-body Efimov parameter) or, alternatively, the lowest energy of the trapped three-boson system at unitarity (this assumes the use of a low-energy Hamiltonian such that the lowest trimer can be described by Efimov's theory if the trap is removed). While we believe that our four-boson spectrum has the same key characteristics—such as the energy-level crossings and spacings as well as

the classification into universal and nonuniversal states—as the ones one would obtain for the zero-range model III, we did not attempt to extrapolate our results to the $r_0 \to 0$ and $R_0 \to 0$ limits. References [52,53] pursued this, finding the values of $-0.1(2)E_{\rm ho}$, $2.7(3)E_{\rm ho}$, and $4.6(5)E_{\rm ho}$ for the lowest three relative four-boson energies, for the lowest relative two- and three-boson energies both fixed at $E_{\rm ho}/2$. Our three lowest four-boson energies (see Table II; due to our finite value of r_0, our two-boson energy is $0.5103E_{\rm ho}$ and not $E_{\rm ho}/2$) lie within the estimated numerical error bars of Ref. [53].

Having a solid understanding of the energy spectrum at unitarity, we consider the finite scattering length regime. We start our discussion in the weakly interacting regime, where the hard-core Bose gas model should provide a reasonable description of the "lowest BEC state." Here, the term lowest BEC state refers to the state that is occupied if the system is initially prepared in a state with $a_s = 0$ and relative energy $9E_{\rm ho}/2$ and if the s-wave scattering length is then increased adiabatically. The $N = 4$ energy of the hard-core model is shown by a solid line in Fig. 3 for $a_{\rm ho}/a_s \geqslant 1.7$. While the smallest $a_{\rm ho}/a_s$ (largest $a_s/a_{\rm ho}$) considered may already be somewhat outside of the validity regime of the hard-core model, the energies for the larger $a_{\rm ho}/a_s$ can be used as a reliable guide for where the BEC state should lie. It can be seen that one of the four-boson states for model II approaches the hard-core model energy with increasing $a_{\rm ho}/a_s$. This state undergoes several avoided crossings. If we diabatize these avoided crossings (we do this by eye), then this state connects with the lowest quasiuniversal state at unitarity. We identify this state as the lowest BEC state. Interestingly, and somewhat surprisingly, the lowest BEC state does not, according to our interpretation, connect to a universal state at unitarity but rather to a quasiuniversal state. The implication is that, in a many-body BEC at unitarity, three-body (or higher-body) parameters may be required to describe the gas.

The lowest state for $v_0 = 0$ and $V_0 = 97\,700E_{\rm ho}$ has an energy of $4.5017E_{\rm ho}$, which is very close to the energy of $9E_{\rm ho}/2$ of the noninteracting system. Taking this state as our initial state and assuming an instantaneous sweep to unitarity, we obtain the occupation probabilities listed in column 7 of Table II. It can be seen that the $(v,q) = (0,0)$ and $(0,1)$ states at unitarity have the largest occupation probabilities. The $(v,q) = (0,0)$ state was identified above as merging into the four-body state tied to the lowest three-body Efimov trimer when the trapping potential goes to zero. Using this, the $(v,q) = (0,1)$ state, which has the largest occupation probability, is best characterized as an "excited four-body state" (breathing mode type excitation) as opposed to a "trimer plus atom state." This observation begs the question whether the N-body short-time dynamics is governed predominantly by three-body Efimov physics (as implicitly implied if the N-body dynamics is modeled by a three-body Hamiltonian) or whether four-body and possibly also higher-body physics plays a non-negligible role, at least for certain parameter combinations.

Figure 6 shows the scaled pair distribution functions $r_{jk}^2 P_{\rm pair}(r_{jk})$, normalized such that $4\pi \int P_{\rm pair}(r_{jk}) r_{jk}^2 dr_{jk} = 1$, of the lowest BEC state for selected a_s for (a) $N = 3$ and (b) $N = 4$. The scattering length values are chosen such that the states identified as the lowest BEC states are isolated (away from avoided crossings). Figure 6 shows that the pair

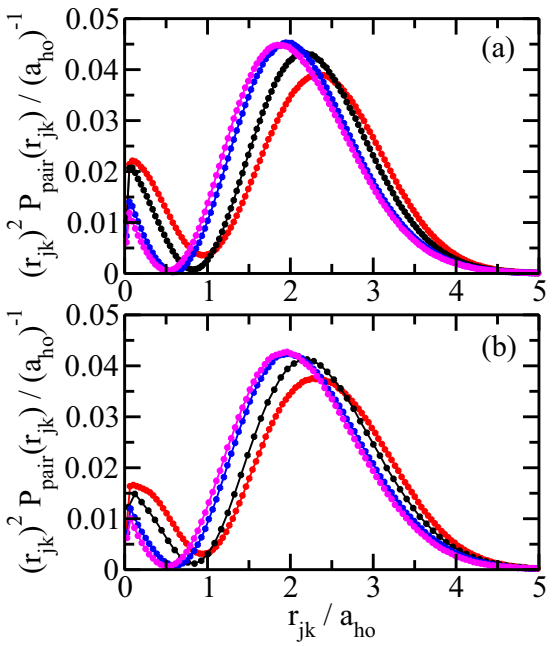

FIG. 6. Scaled pair distribution function $r_{jk}^2 P_{\rm pair}(r_{jk})$ for the lowest BEC state for various a_s for (a) $N = 3$ and (b) $N = 4$. The calculations are for the interaction model II with $V_0 = 97\,700E_{\rm ho}$. The curves from bottom to top at $r_{jk}/a_{\rm ho} = 1.5$ correspond to $a_{\rm ho}/a_s = 0$, $1/2$, $\approx$1.3500, and $\approx$1.7012.

distribution functions for the $N = 3$ and $N = 4$ systems are very similar, with the amplitude at small r_{jk} differing a bit. For the smallest a_s considered, the pair distribution functions go to a very good approximation to zero at $r_{ij} = a_s$. If we assume a Jastrow-type variational wave function that consists of a product over two-body functions, the observed behavior is consistent with the intuitive picture that the lowest BEC state is described by two-body correlation functions that have a node, i.e., that can be interpreted as excited pairs (see also Refs. [31,59]). As a_s increases, the state identified as the lowest BEC state is characterized by a pair distribution function that displays a minimum at r_{jk} values smaller than a_s. This can be thought of as a kind of saturation. Clearly, if a minimum exists it has to be at finite r_{jk} and not at $r_{jk} \to \infty$ as a_s goes to infinity. Interestingly, the minimum of $r_{jk}^2 P(r_{jk})$ does not go to zero but takes on finite values. This suggests that higher-body correlations may play a role in the large a_s limit. We expect that the small r_{jk} behavior of the pair distribution functions for the homogeneous system is qualitatively similar to those diplayed in Fig. 6 for the harmonically trapped systems.

V. SUMMARY AND OUTLOOK

This paper presented a comprehensive study of the harmonically trapped four-boson system interacting through two-body short-range interactions with positive s-wave scattering length a_s, including infinitely large a_s. The two-body interactions were parametrized through a purely attractive two-body Gaussian, which allows—in free space—for the formation of many deeply bound molecular states. To eliminate

deep-lying molecular states and to work in a regime where the free-space four-body energies at unitarity are tied uniquely (i.e., through universal numbers) to the free-space Efimov trimers at unitarity, a purely repulsive three-body Gaussian potential was added. The interaction parameters were adjusted such that the size $L_{\rm fs}$ of the lowest free-space Efimov trimer at unitarity is just a bit larger than the characteristic length $a_{\rm ho}$ of the external spherically symmetric harmonic trapping potential. Correspondingly, the size of the lowest free-space tretramer at unitarity is quite close to $a_{\rm ho}$. Since the "internal" characteristic length scales (sizes of the free-space trimer and tetramer) are comparable to the "external" characteristic length scale (harmonic-oscillator length $a_{\rm ho}$), the chosen parameter combinations are expected to yield a rich energy spectrum. Indeed, the low-energy four-boson energy spectrum for the employed model interaction displays a maze of energy levels and crossings.

Among the many energy levels, we identified—diabatizing, by eye, some of the avoided crossings—one energy level as the lowest gaslike BEC state. While a strict definition of this state was not provided, our working definition was as follows: assuming one prepares the four-boson system in the noninteracting eigenstate and one then increases the s-wave scattering length adiabatically, jumping across narrow avoided crossings quickly, one should follow an energy level whose energy increases monotonically and whose properties depend at most weakly on the three-body interaction employed. While we quantified the three-body contact at unitarity, we did not recalculate the entire four-boson spectrum for a second or third parametrization of the three-body potential, using the same $\kappa^*_{\rm fs}$, i.e., fixing the "internal" scale to the same value. Moreover, this work did not recalculate the four-boson energy spectrum for other $\kappa^*_{\rm fs}$ values. Studying the dependencies on the parametrization of the interactions and systematically varying $\kappa^*_{\rm fs}$ are left for future work. Nevertheless, with the energy spectrum at hand, we were able to extract some information of the lowest gaslike BEC state. In particular, the pair distribution function in the strongly interacting regime acquires a minimum at $r \approx a_{\rm ho}$ but does not go to zero. This finding may provide guidance for constructing improved variational descriptions of the strongly interacting Bose gas.

The paper also presented a comprehensive analysis of the energies of the trapped four-boson system at unitarity. The energy levels were assigned approximate quantum numbers and classified as universal (vanishing three-body contact C_3) and nonuniversal (finite three-body contact C_3). Moreover, depending on the value of C_3, the nonuniversal states were further categorized as "quasiuniversal" and "strongly nonuniversal." The assignment and classification scheme of the four-boson system were corroborated by analyzing structural properties, namely the hyperradial density $P(R)$ and the subhyperradial density $P_{\rm sub}(R)$. Our work suggests that the contacts C_2 and C_3 can be thought of as analogs of quantum numbers in that they provide a classification scheme of the states.

The present work suggests several future research directions. It would be interesting to compare the present energy spectrum with that for other interaction models as well as other $\kappa^*_{\rm fs}$. It would also be interesting to use the four-boson spectrum presented here as a starting point for simulating time ramps, possibly including both three- and four-body loss coefficients. The presented results can be used as benchmarks with which to test approximate variational schemes, collective coordinate approaches, or trial wave functions employed in quantum Monte Carlo studies.

ACKNOWLEDGMENTS

D.B. gratefully acknowledges support by the National Science Foundation through Grants No. PHY-1509892 and No. PHY-1745142 and discussions with Hans-Werner Hammer. M.W.C.S. and J.L.B. acknowledge support from the JILA Physics Frontier Center, Grant No. PHY-1734006.

[1] S. Giorgini, L. P. Pitaevskii, and S. Stringari, Theory of ultracold atomic Fermi gases, Rev. Mod. Phys. **80**, 1215 (2008).

[2] S. Cowell, H. Heiselberg, I. E. Mazets, J. Morales, V. R. Pandharipande, and C. J. Pethick, Cold Bose Gases with Large Scattering Lengths, Phys. Rev. Lett. **88**, 210403 (2002).

[3] G. A. Baker, Jr., Neutron matter model, Phys. Rev. C **60**, 054311 (1999).

[4] F. Werner and Y. Castin, Unitary gas in an isotropic harmonic trap: Symmetry properties and applications, Phys. Rev. A **74**, 053604 (2006).

[5] T.-L. Ho, Universal Thermodynamics of Degenerate Quantum Gases in the Unitarity Limit, Phys. Rev. Lett. **92**, 090402 (2004).

[6] C. A. Regal, M. Greiner, and D. S. Jin, Observation of Resonance Condensation of Fermionic Atom Pairs, Phys. Rev. Lett. **92**, 040403 (2004).

[7] M. W. Zwierlein, C. A. Stan, C. H. Schunck, S. M. F. Raupach, A. J. Kerman, and W. Ketterle, Condensation of Pairs of Fermionic Atoms near a Feshbach Resonance, Phys. Rev. Lett. **92**, 120403 (2004).

[8] L. H. Thomas, The interaction between a neutron and a proton and the structure of H^3, Phys. Rev. **47**, 903 (1935).

[9] V. Efimov, Energy levels arising from resonant two-body forces in a three-body system, Phys. Lett. B **33**, 563 (1970).

[10] E. Braaten and H.-W. Hammer, Universality in few-body systems with large scattering length, Phys. Rep. **428**, 259 (2006).

[11] P. Naidon and S. Endo, Efimov physics: A review, Rep. Prog. Phys. **80**, 056001 (2017).

[12] N. Navon, S. Piatecki, K. Günter, B. Rem, T. C. Nguyen, F. Chevy, W. Krauth, and C. Salomon, Dynamics and Thermodynamics of the Low-Temperature Strongly Interacting Bose Gas, Phys. Rev. Lett. **107**, 135301 (2011).

[13] R. J. Wild, P. Makotyn, J. M. Pino, E. A. Cornell, and D. S. Jin, Measurements of Tan's Contact in an Atomic Bose-Einstein Condensate, Phys. Rev. Lett. **108**, 145305 (2012).

[14] B. S. Rem, A. T. Grier, I. Ferrier-Barbut, U. Eismann, T. Langen, N. Navon, L. Khaykovich, F. Werner, D. S. Petrov, F. Chevy, and C. Salomon, Lifetime of the Bose Gas with Resonant Interactions, Phys. Rev. Lett. **110**, 163202 (2013).

[15] R. J. Fletcher, A. L. Gaunt, N. Navon, R. P. Smith, and Z. Hadzibabic, Stability of a Unitary Bose Gas, Phys. Rev. Lett. **111**, 125303 (2013).
[16] P. Makotyn, C. E. Klauss, D. L. Goldberger, E. A. Cornell, and D. S. Jin, Universal dynamics of a degenerate unitary Bose gas, Nat. Phys. **10**, 116 (2014).
[17] U. Eismann, L. Khaykovich, S. Laurent, I. Ferrier-Barbut, B. S. Rem, A. T. Grier, M. Delehaye, F. Chevy, C. Salomon, L.-C. Ha, and C. Chin, Universal Loss Dynamics in a Unitary Bose Gas, Phys. Rev. X **6**, 021025 (2016).
[18] C. E. Klauss, X. Xie, C. Lopez-Abadia, J. P. D'Incao, Z. Hadzibabic, D. S. Jin, and E. A. Cornell, Observation of Efimov Molecules Created from a Resonantly Interacting Bose Gas, Phys. Rev. Lett. **119**, 143401 (2017).
[19] R. J. Fletcher, R. Lopes, J. Man, N. Navon, R. P. Smith, M. W. Zwierlein, and Z. Hadzibabic, Two- and three-body contacts in the unitary Bose gas, Science **355**, 377 (2017).
[20] B. D. Esry, C. H. Greene, and J. P. Burke, Jr., Recombination of Three Atoms in the Ultracold Limit, Phys. Rev. Lett. **83**, 1751 (1999).
[21] E. Nielsen and J. H. Macek, Low-Energy Recombination of Identical Bosons by Three-Body Collisions, Phys. Rev. Lett. **83**, 1566 (1999).
[22] P. F. Bedaque, E. Braaten, and H.-W. Hammer, Three-body Recombination in Bose Gases with Large Scattering Length, Phys. Rev. Lett. **85**, 908 (2000).
[23] T. Kraemer, M. Mark, P. Waldburger, J. G. Danzl, C. Chin, B. Engeser, A. D. Lange, K. Pilch, A. Jaakkola, H.-C. Nägerl, and R. Grimm, Evidence for Efimov quantum states in an ultracold gas of caesium atoms, Nature (London) **440**, 315 (2006).
[24] J. L. Song and F. Zhou, Ground State Properties of Cold Bosonic Atoms at Large Scattering Lengths, Phys. Rev. Lett. **103**, 025302 (2009).
[25] Y.-L. Lee and Y.-W. Lee, Universality and stability for a dilute Bose gas with a Feshbach resonance, Phys. Rev. A **81**, 063613 (2010).
[26] X. Yin and L. Radzihovsky, Quench dynamics of a strongly interacting resonant Bose gas, Phys. Rev. A **88**, 063611 (2013).
[27] F. Zhou and M. S. Mashayekhi, Bose gases near resonance: Renormalized interactions in a condensate, Ann. Phys. (NY) **328**, 83 (2013).
[28] A. G. Sykes, J. P. Corson, J. P. D'Incao, A. P. Koller, C. H. Greene, A. M. Rey, K. R. A. Hazzard, and J. L. Bohn, Quenching to unitarity: Quantum dynamics in a three-dimensional Bose gas, Phys. Rev. A **89**, 021601(R) (2014).
[29] S. Piatecki and W. Krauth, Efimov-driven phase transitions of the unitary Bose gas, Nat. Commun. **5**, 3503 (2014).
[30] J. P. Corson and J. L. Bohn, Bound-state signatures in quenched Bose-Einstein condensates, Phys. Rev. A **91**, 013616 (2015).
[31] F. Ancilotto, M. Rossi, L. Salasnich, and F. Toigo, Quenched dynamics of the momentum distribution of the unitary bose gas, Few-Body Syst. **56**, 801 (2015).
[32] Y. Yan and D. Blume, Energy and structural properties of N-boson clusters attached to three-body Efimov states: Two-body zero-range interactions and the role of the three-body regulator, Phys. Rev. A **92**, 033626 (2015).
[33] X. Yin and L. Radzihovsky, Postquench dynamics and prethermalization in a resonant Bose gas, Phys. Rev. A **93**, 033653 (2016).
[34] S.-J. Jiang, J. Maki, and F. Zhou, Long-lived universal resonant Bose gases, Phys. Rev. A **93**, 043605 (2016).
[35] Y. Ding and C. H. Greene, Renormalized contact interaction in degenerate unitary Bose gases, Phys. Rev. A **95**, 053602 (2017).
[36] V. E. Colussi, J. P. Corson, and J. P. D'Incao, Dynamics of Three-Body Correlations in Quenched Unitary Bose Gases, Phys. Rev. Lett. **120**, 100401 (2018).
[37] J. Carlson, S. Gandolfi, U. van Kolck, and S. A. Vitiello, Ground-State Properties of Unitary Bosons: From Clusters to Matter, Phys. Rev. Lett. **119**, 223002 (2017).
[38] M. H. Kalos, D. Levesque, and L. Verlet, Helium at zero temperature with hard-sphere and other forces, Phys. Rev. A **9**, 2178 (1974).
[39] S. Giorgini, J. Boronat, and J. Casulleras, Ground state of a homogeneous Bose gas: A diffusion Monte Carlo calculation, Phys. Rev. A **60**, 5129 (1999).
[40] D. Blume and C. H. Greene, Quantum corrections to the ground-state energy of a trapped Bose-Einstein condensate: A diffusion Monte Carlo calculation, Phys. Rev. A **63**, 063601 (2001).
[41] B. L. Hammond, W. A. Lester, Jr., and P. J. Reynolds, *Monte Carlo Methods in Ab Initio Quantum Chemistry*, World Scientific Lecture and Course Notes in Chemistry Vol. 1 (World Scientific, Singapore, 1994).
[42] Y. Suzuki and K. Varga, *Stochastic Variational Approach to Quantum-Mechanical Few-Body Problems*, 1st ed. (Springer-Verlag, Heidelberg, 1998).
[43] J. Mitroy, S. Bubin, W. Horiuchi, Y. Suzuki, L. Adamowicz, W. Cencek, K. Szalewicz, J. Komasa, D. Blume, and K. Varga, Theory and application of explicitly correlated Gaussians, Rev. Mod. Phys. **85**, 693 (2013).
[44] D. Rakshit, K. M. Daily, and D. Blume, Natural and unnatural parity states of small trapped equal-mass two-component Fermi gases at unitarity and fourth-order virial coefficient, Phys. Rev. A **85**, 033634 (2012).
[45] J. Usukura and Y. Suzuki, Resonances of positronium complexes, Phys. Rev. A **66**, 010502(R) (2002).
[46] Y. Castin, Exact scaling transform for a unitary quantum gas in a time dependent harmonic potential, C. R. Phys. **5**, 407 (2004).
[47] S. Tan, Short range scaling laws of quantum gases with contact interactions, arXiv:cond-mat/0412764.
[48] V. N. Efimov, Weakly-bound states of 3 resonantly-interacting particles, Sov. J. Nucl. Phys. **12**, 589 (1971).
[49] V. Efimov, Energy levels of three resonantly interacting particles, Nucl. Phys. A **210**, 157 (1973).
[50] F. Werner and Y. Castin, Unitary Quantum Three-Body Problem in a Harmonic Trap, Phys. Rev. Lett. **97**, 150401 (2006).
[51] S. Jonsell, H. Heiselberg, and C. J. Pethick, Universal Behavior of the Energy of Trapped Few-Boson Systems with Large Scattering Length, Phys. Rev. Lett. **89**, 250401 (2002).
[52] S. Tölle, H.-W. Hammer, and B. C. Metsch, Universal few-body physics in a harmonic trap, C. R. Phys. **12**, 59 (2011).
[53] S. Tölle, H.-W. Hammer, and B. C. Metsch, Convergence properties of the effective theory for trapped bosons, J. Phys. G **40**, 055004 (2013).
[54] J. von Stecher, J. P. D'Incao, and C. H. Greene, Signatures of universal four-body phenomena and their relation to the Efimov effect, Nat. Phys. **5**, 417 (2009).
[55] L. Platter, H.-W. Hammer, and U.-G. Meißner, Four-boson system with short-range interactions, Phys. Rev. A **70**, 052101 (2004).

[56] D. H. Smith, E. Braaten, D. Kang, and L. Platter, Two-body and Three-body Contacts for Identical Bosons Near Unitarity, Phys. Rev. Lett. **112**, 110402 (2014).

[57] D. Blume and C. H. Greene, Three particles in an external trap: Nature of the complete $J = 0$ spectrum, Phys. Rev. A **66**, 013601 (2002).

[58] A. Deltuva, Efimov physics in bosonic atom-trimer scattering, Phys. Rev. A **82**, 040701(R) (2010).

[59] M. W. C. Sze, A. G. Sykes, D. Blume, and J. L. Bohn, Hyperspherical lowest-order constrained-variational approximation to resonant Bose-Einstein condensates, Phys. Rev. A **97**, 033608 (2018).